



Universiteit
Leiden
The Netherlands

Strings and AdS/CFT at finite density

Goykhman, M.

Citation

Goykhman, M. (2014, June 24). *Strings and AdS/CFT at finite density*. *Casimir PhD Series*. Retrieved from <https://hdl.handle.net/1887/26886>

Version: Not Applicable (or Unknown)

License: [Leiden University Non-exclusive license](#)

Downloaded from: <https://hdl.handle.net/1887/26886>

Note: To cite this publication please use the final published version (if applicable).

Cover Page



Universiteit Leiden



The handle <http://hdl.handle.net/1887/26886> holds various files of this Leiden University dissertation

Author: Goykhman, Mikhail

Title: Strings and AdS/CFT at finite density

Issue Date: 2014-06-24

Chapter 3

S-parameter, Technimesons, and Phase Transitions in Holographic Tachyon DBI Models

3.1 Introduction and summary

Systems of strongly interacting fermions have applications in many realms, including condensed matter (e.g. graphene) and particle physics (e.g. technicolor models). A simple way to introduce interaction between fermions involves adding a quartic term to the lagrangian of N free fermions, resulting in the Nambu-Jona-Lasinio model (see e.g. [1] for a review). In three space-time dimensions the model is renormalizable to all orders in the $1/N$ expansion: one can take a double scaling limit where the coupling is tuned to the critical value, while the UV cutoff is sent to infinity, keeping the physical mass fixed. Dynamical mass generation at sufficiently large values of the coupling is an important feature which is believed to happen in other strongly interacting fermion systems.

Unfortunately one often has to resort to approximate methods to describe the physics in the vicinity of the phase transition from the massless phase to the one with a gap. This is because the transition happens at the intermediate values of the coupling where both the weak coupling and strong coupling expansions break down. Nevertheless such description is often very useful for phenomenological reasons: for example, the walking

technicolor models are precisely of this type, since they stay very close to the putative conformal fixed point for the long RG time. In [2] a tachyon dynamics in the AdS space-time was shown to holographically model this type of physics; this has been further studied in [3] in the context of a particular holographic model based on the Tachyon DBI action in AdS. The mass of the tachyon is tuned to the critical value (the BF bound) and at the same time the UV cutoff is sent to infinity, so that the physical scale measured, for example, by the meson masses, stays fixed.

In this chapter we study some phenomenological applications of the model proposed in [3] which, in turn, was motivated by the holographic description of the dynamics of the D3 and D7 branes intersecting along 2+1 dimensions [4]. We restrict our attention to four space-time dimensions. In the next Section we investigate the phase diagram of the holographic model at finite temperature and charge density. We show that the phase transition at finite temperature between the symmetric and the massive phase is generalized into the phase transition line in the temperature-charge density plane. Furthermore, depending on the value of the quartic coefficient in the tachyon potential, the phase transition line can either stay first order, or possess a critical point where the order of the phase transition changes from second to first. This is somewhat similar to the situation with the (conjectural) phase diagram of QCD with massless quarks and constitutes an interesting prediction for the phase diagram of strongly interacting fermions.

In Section 3 we explore a possibility of using the holographic TDBI model in the context of holographic walking technicolor. We couple the tachyon bilinear to the gauge fields in the adjoint representations of $SU(N_f)_L$ and $SU(N_f)_R$ which contain electroweak gauge group (setting $N_f = 2$ and embedding the electroweak group as $SU(2) \times U(1) \subset SU(2)_L \times SU(2)_R$ constitutes the simplest setup). Tachyon condensate breaks electroweak symmetry and generates masses for the W and Z bosons giving rise to a model of holographic walking technicolor. We compute the Peskin-Takeuchi S-parameter for a variety of tachyon potentials and observe that it is positive and does not go to zero. In Section 4 we compute the masses of the lightest scalar technimesons for a certain family of the tachyon potentials and observe that even though there is no parametrically light “technidilaton”, the lowest lying meson can be an order of magnitude lighter than the next one.

We conclude in Section 5. Appendix contains application of the holo-

graphic RG to the holographic tachyon TDBI model, where a picture for the running of the double trace coupling, expected from field theoretic considerations, is reproduced.

3.2 Holographic TDBI at finite temperature and chemical potential

In this Section we consider holographic tachyon DBI model at finite temperature and chemical potential. We consider AdS-Schwarzschild black hole to account for a non-vanishing temperature, and we turn on a background flux of the $U(1)$ gauge potential which corresponds to the finite density in the dual field theory. We describe the phase with broken conformal symmetry by the dual picture with non-vanishing tachyon field in the bulk, while conformally symmetric field theory state corresponds to the identically vanishing tachyon in the bulk. We compute holographically free energies of both phases and determine the resulting phase diagram.

Perhaps the future development of the results of this Section will mostly lie in the realm of condensed matter physics. However, let us make a slight detour and remind the reader a closely related problem, a phase diagram of QCD at finite temperature and chemical potential. (See e.g. [5, 6] for recent reviews). The phase structure of QCD is roughly the following. If the temperature is low and we increase the density, then at some value of the density the system is expected to undergo a first order phase transition to the states where the hadrons dissociate. At sufficiently large density, the system gets into the color superconducting phase. In this phase confined bound state of two quarks goes to Coulomb bound state, in a process similar to Cooper pairing in the microscopic description of a superconductor. Increasing the temperature destroys Cooper pairing mechanism for the quarks, eventually giving rise to a quark-gluon plasma. This is believed to be a preferred high temperature state for any values of the chemical potential, however the phase transition from the hadronic state is first order for larger densities, but second order for smaller densities (for massless quarks). As we will see below, we can observe somewhat similar phase structure for certain TDBI models, though either the orders of first and second order phase transitions are interchanged or we have two critical points at which the order of phase transition changes.

Phase transitions in the holographic tachyon DBI at finite temperature have been studied in [3], which the reader is encouraged to consult

for technical details relevant to the present Section ¹. There it has been established that the order of the phase transition is determined by the behavior of the tachyon potential for very small values of T (the tachyon field). In the BKT limit, where the UV cutoff is taken to infinity, with physical observables held fixed, the solution must have a fixed ratio between the two asymptotics near the boundary of AdS. The value of the coefficient in front of the T^4 term in the tachyon potential determines whether increasing the value of T at the black hole horizon corresponds to the smaller or larger temperatures. In the former case, the transition is second order, while in the latter case it is first order. In the following we repeat this analysis in the presence of finite density.

Consider finite temperature AdS_{d+1} -Schwarzschild metric

$$ds^2 = r^2 \left(-F(r)dt^2 + (dx^1)^2 + \dots + (dx^{d-1})^2 \right) + \frac{dr^2}{r^2 F(r)}, \quad (3.1)$$

where $F(r) = 1 - (\frac{r_h}{r})^d$, and turn on non-vanishing flux \hat{A}_0 . Tachyon-DBI action then takes the form

$$S_{TDBI} = - \int_{r_h}^{\infty} dr \int d^d x r^{d-1} V(T) \sqrt{1 + r^2 \hat{T}^2 F - \hat{A}_0^2}. \quad (3.2)$$

From equation of motion for gauge flux we obtain

$$\hat{A}_0^2 = \frac{\hat{d}^4 (1 + r^2 F \hat{T}^2)}{r^{2(d-1)} V^2 + \hat{d}^4}, \quad (3.3)$$

where $\hat{d}(\mu_{ch}, r_h)$ is a constant of integration. As usual, up to a normalization constant, \hat{d}^2 is proportional to the charge density of the system. Due to (3.3) in the leading order in T we obtain

$$\begin{aligned} \mu_{ch} &= \int_{r_h}^{\infty} \frac{dr \hat{d}^2}{\sqrt{\hat{d}^4 + r q n 2(d-1)}} \\ &= \frac{\hat{d}^2}{(d-2)r_h^{d-2}} {}_2F_1 \left(\frac{1}{2}, \frac{d-2}{2(d-1)}, \frac{3d-4}{2(d-1)}, -\frac{\hat{d}^4}{r_h^{2(d-1)}} \right). \end{aligned} \quad (3.4)$$

¹In recent work [7] the phase structure of the holographic model of QCD in the Veneziano limit has been analyzed at finite temperature.

Plugging (3.3) in into the action (3.2) we arrive at

$$S_{TDBI} = - \int_{r_h}^{\infty} dr \int d^d x r^{2(d-1)} V^2 \left((1+r^2 F \dot{T}^2) (r^{2(d-1)} V^2 + \hat{d}^4)^{-1} \right)^{1/2}. \quad (3.5)$$

Introduce dimensionless coordinate, $\tilde{r} = r/\hat{d}^{\frac{2}{d-1}}$, and dimensionless temperature, $\tilde{r}_h = r_h/\hat{d}^{\frac{2}{d-1}}$. As a result the action acquires the form

$$S_{TDBI} = -\hat{d}^{\frac{2d}{d-1}} \int_{\tilde{r}_h}^{\infty} d\tilde{r} \int d^d x \frac{\tilde{r}^{2(d-1)} V^2}{\sqrt{1 + \tilde{r}^{2(d-1)} V^2}} \sqrt{1 + \tilde{r}^2 F T'^2}, \quad (3.6)$$

where $F = 1 - (\tilde{r}_h/\tilde{r})^d$ and $T' = \partial T/\partial \tilde{r}$.

Let us define tachyon T value at the horizon, $T_h = T(r_h)$. Equation of motion for the tachyon field, following from the action (3.6), is

$$\frac{\partial}{\partial r} \left[\frac{\tilde{r}^{2d} F V^2 T'}{\sqrt{(1 + \tilde{r}^2 F T'^2)(1 + \tilde{r}^{2(d-1)} V^2)}} \right] - \tilde{r}^{2(d-1)} V^2 \frac{2 + \tilde{r}^{2(d-1)} V^2}{(1 + \tilde{r}^{2(d-1)} V^2)^{3/2}} \sqrt{1 + \tilde{r}^2 F T'^2} \partial_T \log V = 0. \quad (3.7)$$

Using (3.7) and imposing the boundary condition $T(\tilde{r} = \tilde{r}_h) = T_h$, we find

$$T'(\tilde{r} = \tilde{r}_h) = \frac{2 + \tilde{r}_h^{2(d-1)} V^2(T_h)}{d\tilde{r}_h(1 + \tilde{r}_h^{2(d-1)} V^2(T_h))} \partial_T \log V(T_h). \quad (3.8)$$

When $T \sim T_h \ll 1$ and $m \simeq m_{BF}^2 = -d^2/4$ we obtain linearized equation of motion

$$\left(\frac{\tilde{r}^{2d} F T'}{\sqrt{1 + \tilde{r}^{2(d-1)} V^2}} \right)' + \frac{d^2 \tilde{r}^{2(d-1)}}{4} \frac{2 + \tilde{r}^{2(d-1)} V^2}{(1 + \tilde{r}^{2(d-1)} V^2)^{3/2}} T = 0 \quad (3.9)$$

and boundary conditions

$$T(\tilde{r} = \tilde{r}_h) = T_h, \quad T'(\tilde{r} = \tilde{r}_h) = -\frac{dT_h}{4\tilde{r}_h} \frac{2 + \tilde{r}_h^{2(d-1)} V^2}{1 + \tilde{r}_h^{2(d-1)} V^2}. \quad (3.10)$$

Near the boundary $\tilde{r} \rightarrow \infty$ behavior of $T(\tilde{r})$ is given by equation

$$T'' + \frac{d+1}{\tilde{r}} T' + \frac{d^2}{4\tilde{r}^2} T = 0. \quad (3.11)$$

Let us now specialize to $d = 4$ case. Near-boundary behavior is then described by equation

$$T'' + \frac{5}{\tilde{r}}T' + \frac{4}{\tilde{r}^2}T = 0. \quad (3.12)$$

which is solved by

$$T(\tilde{r}) \simeq \frac{1}{\tilde{r}^2} (c_1 \log \tilde{r} + c_2) \quad \Rightarrow \quad T(r) = \frac{1}{r^2} \left(c_1 \log \frac{r}{\hat{d}^{2/3}} + c_2 \right). \quad (3.13)$$

Let us denote

$$g = \hat{d}^{2/3} \quad (3.14)$$

The constants c_1 and c_2 can be determined by solving equation of motion (3.7) numerically. If we consider instead linearized equation (3.9) in BKT limit with boundary conditions (3.10), we obtain c_2/c_1 , which is a function of $\tilde{r}_h = r_h/g$. In the case of vanishing temperature and vanishing chemical potential the near-boundary behavior of tachyon field is given by

$$T(r) = \frac{1}{r^2} \left(C_1 \log \frac{r}{\mu} + C_2 \right) \quad (3.15)$$

Clearly it must be the same as (3.13). Matching these equations, we obtain

$$\frac{g}{\mu} = C_0 \exp \left(\Xi \left(\frac{r_h/\mu}{g/\mu} \right) \right), \quad (3.16)$$

where we have denoted $C_0 = e^{-C_2/C_1}$ and $\Xi = c_2/c_1$. Equation (3.16) can be solved numerically, which gives critical values of temperature r_h and g measured in units of μ . The result appears in figure 1. We have checked that when $\hat{d} = 0$ the critical temperature is equal to $2C_0$, which is a correct limiting value [3].

To determine which state in the canonical ensemble is preferred, we need to compare the free energies. Similarly to [3], we focus on the near-critical region, where tachyon field is either vanishing or small. The difference in free energies between non-vanishing tachyon and vanishing tachyon phases is given by

$$\mathcal{F}(r_h, \hat{d}) = S_{TDBI}(T \equiv 0) - S_{TDBI}(T), \quad (3.17)$$

where the last term in the r.h.s. is evaluated on the solution, satisfying $T(r = r_h) = T_h$ boundary condition. Due to $V(0) = 1$ one obtains, using

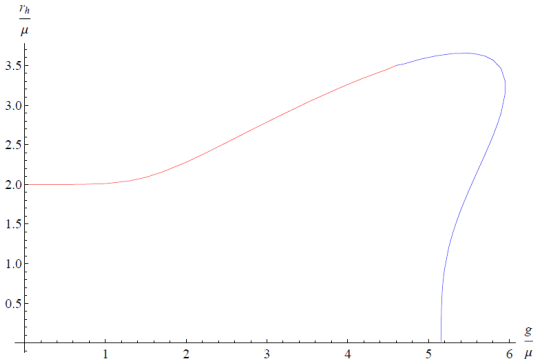


Figure 3.1. Phase diagram for conformal phase transition in $(g/\mu, r_h/\mu)$ plane. Order of phase transition changes at the point $\tilde{r}_h \equiv r_h/g = 0.75$. Blue part of the curve describes second order phase transition and red part of the curve describes first order phase transition.

(3.6)

$$\mathcal{F}(r_h, \hat{d}) = \hat{d}^{8/3} \int_{\tilde{r}_h}^{\infty} d\tilde{r} \int d^4x \tilde{r}^6 \left(\frac{V^2}{\sqrt{1 + \tilde{r}^6 V^2}} \sqrt{1 + \tilde{r}^2 F T'^2} - \frac{1}{\sqrt{1 + \tilde{r}^6}} \right). \quad (3.18)$$

We will need the form of the tachyon potential near $T = 0$:

$$V(T) = 1 + \frac{1}{2} m^2 T^2 + \frac{a}{4} T^4 + \dots, \quad (3.19)$$

where $m^2 \simeq m_{BF}^2 = -4$ and a is the coefficient of the quartic term which, as explained in [3], determines the order of the phase transition in the case of vanishing density. Below we will see that at finite density the situation is more subtle, and the first order phase transition line can join the second order phase transition line at a critical point, provided the value of a is chosen accordingly.

In the BKT limit we have $T \sim T_h \ll 1$ and $m^2 = m_{BF}^2 = -4$. We compute (3.18) up to the fourth order in T_h ,

$$\mathcal{F}(r_h, \hat{d}) = \mathcal{F}_2(r_h, \hat{d}) + \mathcal{F}_4(r_h, \hat{d}) + \dots, \quad (3.20)$$

where

$$\mathcal{F}_2 = \hat{d}^{8/3} \int_{\tilde{r}_h}^{\infty} d\tilde{r} \int d^4x \frac{1}{2\sqrt{1+\tilde{r}^6}} \left(\tilde{r}^8 F T'^2 - 4\tilde{r}^6 \frac{2+\tilde{r}^6}{1+\tilde{r}^6} T^2 \right)$$

$$\mathcal{F}_4 = -\hat{d}^{8/3} \int_{\tilde{r}_h}^{\infty} d\tilde{r} \int d^4x \frac{\tilde{r}^6}{8(1+\tilde{r}^6)^{5/2}} \left(F^2 T'^4 \tilde{r}^4 (1+\tilde{r}^6)^2 + \right. \quad (3.21)$$

$$+ 8F\tilde{r}^2 T^2 T'^2 (1+\tilde{r}^6)(2+\tilde{r}^6) + 2T^4 (8(\tilde{r}^6-2) - a(1+\tilde{r}^6)(2+\tilde{r}^6)) \left. \right) \quad (3.22)$$

The quadratic terms vanish on shell, up to the boundary term, which also vanishes, because

$$F(\tilde{r} = \tilde{r}_h) = 0, \quad T(\tilde{r} = \infty) = 0. \quad (3.23)$$

We solve numerically equation (3.9) with boundary conditions (3.10), for each particular $\tilde{r}_h = r_h/g$. This gives us $T = T_1$, which is a solution of the first order in T_h . The first correction to this solution is obtained when we take into account quartic in T_h terms in the action for T , and therefore the corrected solution is $T = T_1 + T_3$, where T_3 is of the third order in T_h . Therefore we need to compute in the leading order

$$\mathcal{F}(T_1 + T_3) = \mathcal{F}_2(T_1 + T_3) + \mathcal{F}_4(T_1 + T_3). \quad (3.24)$$

For brevity let us rewrite (3.70) as

$$\mathcal{F}_2 = \int dr [\alpha(r)T^2 + \beta(r)T'^2]$$

$$\mathcal{F}_4 = \int dr [a(r)T^4 + b(r)T^2 T'^2 + c(r)T'^4]. \quad (3.25)$$

Let us use integration by parts to bring $\mathcal{F}_{2,4}$ to the form

$$\mathcal{F}_2 = \int dr T [\alpha T - (\beta T')'] \equiv \int dr T P_1$$

$$\mathcal{F}_4 = \int dr T \left[aT^3 + \frac{b}{2} T T'^2 - \left(\frac{b}{2} T' T^2 \right)' - (c T'^3)' \right] \equiv \int dr T P_3 \quad (3.26)$$

where $P_{1,3}$ are polynomials of the T , T' , T'' of the degree specified by the subscript. From the variation

$$\delta\mathcal{F} = 2 \int dr \delta T [\alpha T - (\beta T')'] + 4 \int dr \delta T \left[aT^3 + \frac{b}{2} T T'^2 - \left(\frac{b}{2} T' T^2 \right)' - (c T'^3)' \right] \quad (3.27)$$

we obtain equation of motion

$$2P_1(T_1 + T_3) + 4P_3(T_1 + T_3) = 0, \quad (3.28)$$

which we can solve perturbatively as

$$P_1(T_1) = 0, \quad P_1(T_3) + 2P_3(T_1) = 0. \quad (3.29)$$

Using these equations in the expansion of (3.24)

$$\begin{aligned} \mathcal{F} &= \int dr (T_1 + T_3) P_1(T_1 + T_3) + (T_1 + T_3) P_3(T_1 + T_3) \\ &= \int dr T_1 P_1(T_3) + T_3 P_1(T_1) + T_1 P_3(T_1) + \dots \end{aligned} \quad (3.30)$$

we obtain

$$\mathcal{F}(T) \simeq - \int dr T_1 P_3(T_1) = -\mathcal{F}_4(T_1). \quad (3.31)$$

We then evaluate quartic terms, $\mathcal{F}_4(\hat{d}, a)$, on the numerically found solution T_1 . Equation $\mathcal{F}_4(\tilde{r}_h, a) = 0$ gives values of ratio $r_h/g = \tilde{r}_h$ for each particular a at which order of phase transition changes. This equation is valid only for those values of r_h and \hat{d} which are close to critical ones. We solve this equation numerically for each particular value of the parameter a , that is we find $\tilde{r}_h^{(c)}(a)$. The result is plotted in figure 2. Notice that when \hat{d} is sent to zero, \tilde{r}_h goes to infinity, and the special value $a \simeq 6.47$ becomes the same as in the case of vanishing chemical potential [3]. Also notice that when $6.47 \leq a \leq 7.03$ there are two points \tilde{r}_h at which the order of phase transition changes.

In figure 1 we have taken $a = 6.41$ for which phase transition is the second order one for $\frac{r_h}{g} < 0.75$ and the first order one for $\frac{r_h}{g} > 0.75$. This corresponds respectively to the blue and red parts of the phase transition curve in figure 1. ²

The other option is to take the value of a at which we have two critical points where the order of phase transition changes. Then for the temperature bellow some critical value, $\tilde{r}_h^{(c)} < r_h^{(c,1)}$ we have second order phase

²One may use the top-down approach based on the $D3 - D7$ system to derive the phase diagram of $N = 4$ super Yang-Mills coupled to $N = 2$ matter at finite temperature and chemical potential. It also exhibits the phase transition of the second order at small temperatures. See [8] for a recent discussion.

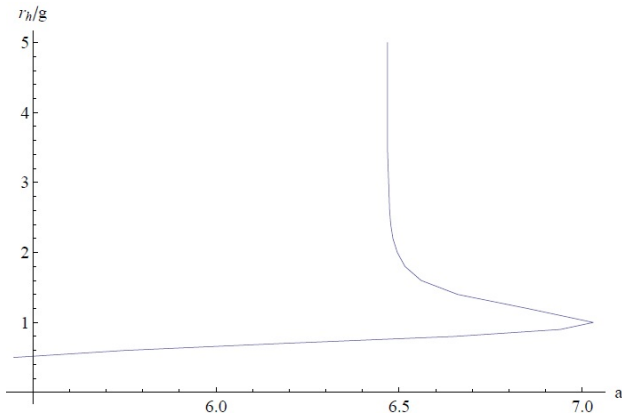


Figure 3.2. The ratio $\tilde{r}_h = r_h/g$ at which the order of phase transition changes, as a function of UV parameter a . It is determined by the sign of \mathcal{F}_4 in the conformal symmetry broken phase. On the left side of the curve $\mathcal{F}_4 < 0$ and phase transition is of the first order, on the right side $\mathcal{F}_4 > 0$ and phase transition is of the second order.

transition, for $\tilde{r}_h^{(c,1)} < \tilde{r}_h^{(c)} < \tilde{r}_h^{(c,2)}$ we have first order order phase transition, and finally for $\tilde{r}_h^{(c)} > \tilde{r}_h^{(c,2)}$ we have second order phase transition. The critical point $\tilde{r}_h^{(c,2)}$ therefore resembles the one in the QCD phase diagram.

As emphasized in [3], the behavior of the free energy for small values of the tachyon condensate determines the order of the phase transition, provided the phase diagram has a simple form. This was the case in all examples studied in [3]. We believe this remains true once the finite density is turned on, but to show this some further numerical work is necessary.

3.3 S parameter

3.3.1 Review of technicolor and S, T, U parameters

Consider the system of 2 techniquark matter fields (\tilde{u}, \tilde{d}) with color charges, transforming in fundamental representation of the gauge group $SU(N_c)$. Quark fields are coupled to gauge field in the adjoint representation of the gauge group. In the ultraviolet regime these quarks are massless, and therefore the system possesses the $SU(2)_L \times SU(2)_R$ chiral symme-

try. Therefore we can couple the doublet of left quarks $Q = (\tilde{u}_L, \tilde{d}_L)$ to bosons of weak gauge group $SU(2)_L$, leaving 2 right quarks \tilde{u}_R and \tilde{d}_R in the singlet representation sector of the weak gauge transformations. We also give each quark field the hypercharge Y , characterizing its representation under the action of the $U(1)_Y$ gauge group.

We look at introduced 2 quarks as a set of strongly-interacting fermionic fields of the physics beyond the Standard Model. At some energy scale due to the strong interaction these quarks may form a chiral condensate, breaking the chiral symmetry down to $SU(2)_{diag}$.³ In the vacuum with spontaneously broken chiral symmetry the 2 quarks acquire a mass. In the technicolor models the phenomenon of the chiral symmetry breaking via techniquark condensation is used to explain the spontaneous electro-weak symmetry breaking, realized therefore as a dynamical symmetry breaking. Furthermore, the extended technicolor models combine these 2 techniquarks with SM matter fields in some specific multiplets in such a way that condensation of techniquarks gives masses to SM matter fields. In the simplest technicolor models such quartic fermionic terms, generated at high scale Λ_{ETC} , lead to flavor changing neutral currents matrix elements that are way above experimental bounds. A walking technicolor models, where the system spends a long RG time in a vicinity of a putative RG fixed point and the anomalous dimension of the technimeson condensate $\gamma \simeq 1$, has been proposed to alleviate this problem. (See [10] for a recent review of walking technicolor and references therein). The theory is necessarily strongly coupled, and it is natural to use holography in this context.

To create a possibility for experimental tests of theories describing physics beyond the Standard Model, Pesking and Takeuchi [11, 12] introduced dimensionless parameters S , T , U , measuring an impact of a hidden sector of heavy beyond-SM fundamental matter fields coupled to electro-weak gauge bosons. They argued (following [13]) that the most important impact arises from oblique corrections: vacuum polarization diagrams, which renormalize gauge boson propagators. Peskin-Takeuchi parameters are expressed via these vacuum polarization amplitudes, and we will review their argument in a greater detail below. For each beyond-SM theory we therefore may compute S , T , U parameters and see whether the results lie within the boundaries set by the deviation of experimental

³It was shown in [9] that under general assumptions in large- N_c chromodynamics the chiral symmetry breaks spontaneously.

data from Standard Model predictions.

The quantum corrections of matter fields to the propagators of the SM gauge fields come from the vacuum polarization amplitudes

$$\int d^4x e^{iq \cdot x} \langle J_a^\mu(x) J_b^\nu(0) \rangle = -i \left(g^{\mu\nu} - \frac{q^\mu q^\nu}{q^2} \right) \Pi_{ab}(q^2), \quad (3.32)$$

where $a, b = 1, 2, 3, Q$ and we are assuming mostly plus signature of the metric. The expression (3.32) should be computed for the matter fields of the SM and for the hidden matter sector of the beyond-SM physics.

For weak currents $J_i, i = 1, 2$, weak isospin current J_3 and electromagnetic current J_Q we have the vacuum polarization amplitudes

$$\Pi_{11}, \Pi_{22}, \Pi_{33}, \Pi_{3Q}, \Pi_{QQ}. \quad (3.33)$$

If we know these amplitudes, then using expression for the electroweak interaction Lagrangian

$$L = \frac{e}{\sqrt{2}s} \left(W_\mu^+ J_\mu^+ + W_\mu^- J_\mu^- \right) + \frac{e}{sc} Z_\mu \left(J_3^\mu - s^2 J_Q^\mu \right) + e A_\mu J_Q^\mu \quad (3.34)$$

we can obtain 1PI self-energies for the electroweak gauge bosons, and 1PI mixing for Z -boson and photon,

$$\Pi_{AA} = e^2 \Pi_{QQ}, \quad \Pi_{ZA} = \frac{e^2}{sc} (\Pi_{3Q} - s^2 \Pi_{QQ}), \dots \quad (3.35)$$

Then with the help of Schwinger-Dyson equations we can derive full quantum propagators for the electroweak gauge fields.

Now, in the interaction Lagrangian (3.34) we have parameters e and

$$s^2 \equiv \sin^2 \theta_W = 1 - \frac{m_W^2}{m_Z^2}. \quad (3.36)$$

Quantum corrections due to the vacuum polarization amplitudes boil down to the renormalization of these parameters,

$$e_\star^2(q^2) \equiv \frac{e^2}{1 - e^2 \Pi_{QQ}(q^2)}, \quad (3.37)$$

$$s_\star^2(q^2) \equiv s^2 - sc \frac{\Pi_{ZA}(q^2)}{q^2 - \Pi_{AA}(q^2)}. \quad (3.38)$$

Then, the renormalized parameter s_* enters the measured left-right Z -decay asymmetry,

$$A_{LR}(q^2) = \frac{2(1 - 4s_*^2)}{1 + (1 - 4s_*^2)^2}, \quad (3.39)$$

and therefore the renormalization of the gauge fields propagators (coming mainly as the oblique corrections due to loops of heavy fermions) can be measured experimentally.

Let us also define θ_0 as

$$\sin(2\theta_0) = \sqrt{\frac{4\pi\alpha_{*,0}(m_Z^2)}{\sqrt{2}G_F m_Z^2}}. \quad (3.40)$$

Here m_Z and G_F are experimentally measured. And $\alpha_{*,0}(m_Z^2)$ is a running electromagnetic coupling, which is computed due to known physics up to $q^2 = m_Z^2$ scale. The running starts from the measured $\alpha(q^2 = 0) = e^2/(4\pi)$.

The renormalization comes from SM and from physics beyond the SM. In the SM the most important contribution comes from t -quark loops (see e.g. [14] Chapter 21),

$$s^2 - s_*^2 = -\frac{3\alpha c^2}{16\pi s^2} \frac{m_t^2}{m_Z^2}, \quad (3.41)$$

$$s_*^2 - s_0^2 = -\frac{3\alpha}{16\pi(c^2 - s^2)} \frac{m_t^2}{m_Z^2}. \quad (3.42)$$

Let us now describe quantum corrections due to vacuum polarization diagrams of beyond-SM physics. First of all for heavy fermion we can expand vacuum polarization amplitudes around $q^2 = 0$,

$$\Pi_{QQ}(q^2) = q^2 \Pi'_{QQ}(0), \quad \Pi_{3Q}(q^2) = q^2 \Pi'_{3Q}(q^2), \quad (3.43)$$

$$\Pi_{33}(q^2) = \Pi_{33}(0) + q^2 \Pi'_{33}(0), \quad (3.44)$$

$$\Pi_{11}(q^2) = \Pi_{11}(0) + q^2 \Pi'_{11}(0), \quad (3.45)$$

where prime denotes differentiation w.r.t. q^2 and we have made use of the fact that Ward identity for electromagnetic field ensures $\Pi_{QQ}(0) = 0$ and $\Pi_{3Q}(0) = 0$. Also we have $\Pi_{11} = \Pi_{22}$. We have therefore six parameters defining vacuum polarization amplitudes of heavy fermions. We make a

renormalization, fixing values of three well-measured parameters, which are α , G_F and m_Z . Three parameters which are left are free of UV divergencies, and we combine these into

$$\alpha S = 4e^2 \left(\Pi'_{33}(0) - \Pi'_{3Q}(0) \right), \quad (3.46)$$

$$\alpha T = \frac{e^2}{s^2 c^2 m_Z^2} \left(\Pi_{11}(0) - \Pi_{33}(0) \right), \quad (3.47)$$

$$\alpha U = 4e^2 \left(\Pi'_{11}(0) - \Pi'_{33}(0) \right). \quad (3.48)$$

In addition to SM corrections (3.41) and (3.42) we can write down contribution of beyond-SM physics via these parameters:

$$\frac{m_W^2}{m_Z^2} - c_0^2 = \frac{\alpha c^2}{c^2 - s^2} \left(-\frac{1}{2} S + c^2 T + \frac{c^2 - s^2}{4s^2} U \right), \quad (3.49)$$

$$s_*^2 - s_0^2 = \frac{\alpha}{c^2 - s^2} \left(\frac{1}{4} S - s^2 c^2 T \right). \quad (3.50)$$

Thus we explicitly constructed a set of experimentally measured quantities, quantum corrections to which may be separately computed from the SM, (3.41), (3.42), and from a hidden sector, (3.49), (3.50), with the latter being expressed via Peskin-Takeuchi parameters. Let us use vector and axial-vector isospin currents

$$J_V^\mu = \bar{\psi} \gamma^\mu \tau_3 \psi, \quad J_A^\mu = \bar{\psi} \gamma^\mu \gamma^5 \tau_3 \psi, \quad (3.51)$$

to express left isospin current as

$$J_3^\mu = \frac{1}{2} (J_V^\mu - J_A^\mu). \quad (3.52)$$

Consider also electromagnetic current, expressed via isospin and hypercharge currents in a usual way,

$$J_Q^\mu = J_V^\mu + \frac{1}{2} J_Y^\mu. \quad (3.53)$$

Assuming the conservation of parity by technicolor interactions we can express isospin current correlator via vector and axial vector isospin correlators, $\Pi_{33} = \frac{1}{4} (\Pi_{VV} + \Pi_{AA})$. We also note that due to isospin conservation $\langle J_3 J_Y \rangle = 0$ (otherwise in technicolor models there would have been a preferred isospin direction), we obtain $\Pi_{3Q} = \frac{1}{2} \Pi_{VV}$. Therefore

$$S = -4\pi (\Pi'_{VV}(q^2) - \Pi'_{AA}(q^2))|_{q^2=0}. \quad (3.54)$$

The holographic tachyon DBI was introduced in [3] to describe a system of strongly interacting fermions, which can be made into the walking technicolor theory. However for the purpose of computing the S-parameter and technimeson masses, we do not even need to specify that the holographic TDBI model describes strongly interacting fermions. Instead, it is sufficient to treat the holographic model as a black box, which produces two-point functions for the vector and axial currents and features spontaneous breaking of the axial symmetry. Then, these currents are coupled to the SM gauge fields to produce spontaneous symmetry breaking of the electroweak gauge group. The resulting contribution to the S-parameter is given by (3.54) and is computed below.

3.3.2 Computation of the S parameter from the tachyon DBI action

As pointed out above, the holographic tachyon DBI theory provides a natural model of the walking technicolor scenario. The important feature of the holographic approach is that we can isolate the impact of beyond-SM sector of the theory. For this purpose we just have to consider a corresponding set of fields in the bulk, and study its classical dynamics⁴.

We need to construct a dual to a strongly interacting theory with the $SU(2)_L \times SU(2)_R$ global symmetry in the UV. The global currents $j_\mu^{(L)}$ and $j_\mu^{(R)}$ give rise to the bulk fields $A_M^{(L,R)}$, living in adjoint of $SU(2)_{L,R}$, with gauge transformations

$$A_M^{(L)} \rightarrow U_L A_M^{(L)} U_L^\dagger + i\partial_M U_L U_L^\dagger, \quad A_M^{(R)} \rightarrow U_R A_M^{(R)} U_R^\dagger + i\partial_M U_R U_R^\dagger. \quad (3.55)$$

Tachyon field $T(r, x)$ lives in bi-fundamental of $SU(2)_L \times SU(2)_R$, i.e., its gauge transformations are given by

$$T \rightarrow U_L T U_R^\dagger. \quad (3.56)$$

Tachyon action with $SU(2)_L \times SU(2)_R$ local symmetry in the bulk is then

$$S = - \int d^4x dr \operatorname{Tr} V(|T|) \left(\sqrt{-G^{(L)}} + \sqrt{-G^{(R)}} \right), \quad (3.57)$$

⁴Previous work dedicated to holographic technicolor and S parameter includes [15–46]; see also [47–53] for recent related work.

where

$$\begin{aligned} G_{MN}^{(R)} &= G_{MN} + F_{MN}^{(R)}, & G_{MN} &= g_{MN} + (D_{(M}T)^\dagger D_{N)}T, \\ G^{(R)} &= \det G_{MN}^{(R)}, \end{aligned} \quad (3.58)$$

and similar for the left; and covariant derivative of tachyon field is given by

$$D_M T = \partial_M T + iA_M^{(L)} T - iTA_M^{(R)}. \quad (3.59)$$

Similar actions for the tachyon have been introduced in [54].

We have $A_M^{(L,R)} = (A_r^{(L,R)}, A_\mu^{(L,R)})$ and we partly fix the gauge symmetry putting

$$A_r^{(L)} = 0, \quad A_r^{(R)} = 0. \quad (3.60)$$

Let us introduce gauge fields in the bulk, dual to vector and axial currents on the boundary:

$$A_M^{(L)} = \frac{1}{2}(V_M - A_M), \quad A_M^{(R)} = \frac{1}{2}(V_M + A_M) \quad (3.61)$$

Suppose we have background tachyon field $T(r) = \langle T(r) \rangle I$, with real-valued vacuum average $\langle T(r) \rangle = T_0(r)$, satisfying equation of motion at vanishing gauge fields,

$$\frac{d}{dr} \left(\frac{r^5 \dot{T}_0}{\sqrt{1 + r^2 \dot{T}_0^2}} \right) = \frac{r^3 \partial_T \log V(T_0)}{\sqrt{1 + r^2 \dot{T}_0^2}} \quad (3.62)$$

Such a background tachyon field breaks the symmetry down to $SU(2)_{diag}$, which means $U_L = U_R$. Its non-zero covariant derivative components, due to the gauge choice (3.60) and definition (3.61) are (the fact that T couples only to axial field A means that axial symmetry is broken)

$$D_r T = \dot{T}_0 I, \quad D_\mu T = -iA_\mu T_0. \quad (3.63)$$

In what follows we consider the case of just one flavor of quark fields. The results can be generalized to arbitrary number of flavors, because for the holographic computation of two-point functions higher order non-abelian terms in gauge field Lagrangian do not play any role. We therefore have

$$G_{MN} = g_{MN} + \partial_M T_0 \partial_N T_0 + A_M A_N T_0^2. \quad (3.64)$$

Let us denote for brevity

$$\mathcal{G}_{MN} = g_{MN} + \partial_M T_0 \partial_N T_0 = \text{diag} \left(-r^2, r^2, r^2, r^2, \frac{1+r^2 \dot{T}_0^2}{r^2} \right), \quad (3.65)$$

and let us write down an inverse matrix to (3.65)

$$\mathcal{M}^{MN} \equiv (\mathcal{G}^{-1})^{MN} = \text{diag} \left(-\frac{1}{r^2}, \frac{1}{r^2}, \frac{1}{r^2}, \frac{1}{r^2}, \frac{r^2}{1+r^2 \dot{T}_0^2} \right). \quad (3.66)$$

We also denote

$$\sqrt{-G} = \sqrt{-\det \|G_{MN}\|}, \quad (3.67)$$

$$\sqrt{-G_0} = \sqrt{-\det \|\mathcal{G}_{MN}\|} = r^3 \sqrt{1+r^2 \dot{T}_0^2},$$

$$K_{MN} = G_{MN} - \mathcal{G}_{MN} = A_M A_N T_0^2. \quad (3.68)$$

Up to second order in A we expand

$$\begin{aligned} \sqrt{-G} &= \sqrt{-G_0} \exp \left(\frac{1}{2} \text{tr} \log(1 + \mathcal{M}K) \right) \\ &= r^3 \sqrt{1+r^2 \dot{T}_0^2} \left(1 + \frac{T_0^2}{2r^2} \eta^{\mu\nu} A_\mu A_\nu \right). \end{aligned} \quad (3.69)$$

Expanding action (3.57) up to second power of gauge fields and replacing left and right gauge fields with vectors and axials we get

$$\begin{aligned} S &= - \int d^4 x dr V(T_0) \sqrt{-G} \left(2 + \frac{1}{4} (G^{-1})^{M_1 M_2} (G^{-1})^{N_1 N_2} \left(F_{M_1 N_1}^{(L)} F_{M_2 N_2}^{(L)} \right. \right. \\ &\quad \left. \left. + F_{M_1 N_1}^{(R)} F_{M_2 N_2}^{(R)} \right) \right) \\ &= - \int d^4 x dr V(T_0) r^3 \sqrt{1+r^2 \dot{T}_0^2} \left[2 + \frac{T_0^2}{r^2} \eta^{\mu\nu} A_\mu A_\nu \right. \\ &\quad \left. + \frac{1}{8} \mathcal{M}^{M_1 M_2} \mathcal{M}^{N_1 N_2} \left(F_{M_1 N_1}^{(V)} F_{M_2 N_2}^{(V)} + F_{M_1 N_1}^{(A)} F_{M_2 N_2}^{(A)} \right) \right]. \end{aligned} \quad (3.70)$$

Using expression (3.66) for \mathcal{M} and throwing away what is independent of gauge fields we proceed to

$$\begin{aligned} S &= - \int d^4 x dr V(T_0) r^3 \sqrt{1+r^2 \dot{T}_0^2} \left[\frac{1}{4(1+r^2 \dot{T}_0^2)} \eta^{\mu\nu} (\dot{V}_\mu \dot{V}_\nu + \dot{A}_\mu \dot{A}_\nu) \right. \\ &\quad \left. + \frac{1}{8r^4} \eta^{\mu\nu} \eta^{\lambda\rho} \left(F_{\mu\lambda}^{(V)} F_{\nu\rho}^{(V)} + F_{\mu\lambda}^{(A)} F_{\nu\rho}^{(A)} \right) + \frac{T_0^2}{r^2} \eta^{\mu\nu} A_\mu A_\nu \right]. \end{aligned} \quad (3.71)$$

We now go to momentum representation,

$$\begin{aligned} V_\mu(x, r) &= \int \frac{d^4 q}{(2\pi)^2} V_\mu(q, r) e^{-iq_\lambda x^\lambda}, \\ A_\mu(x, r) &= \int \frac{d^4 q}{(2\pi)^2} A_\mu(q, r) e^{-iq_\lambda x^\lambda}, \end{aligned} \quad (3.72)$$

which results in

$$\begin{aligned} S = & - \int d^4 q dr V(T_0) r^3 \sqrt{1+r^2 \dot{T}_0^2} \left[\frac{1}{4(1+r^2 \dot{T}_0^2)} \eta^{\mu\nu} (\dot{V}_\mu \dot{V}_\nu + \dot{A}_\mu \dot{A}_\nu) \right. \\ & \left. + \frac{q^2}{4r^4} \left(V_\mu V_\nu \left(\eta^{\mu\nu} - \frac{q^\mu q^\nu}{q^2} \right) + A_\mu A_\nu \left(\eta^{\mu\nu} \left(1 + \frac{4T_0^2 r^2}{q^2} \right) - \frac{q^\mu q^\nu}{q^2} \right) \right) \right], \end{aligned} \quad (3.73)$$

where all squared gauge fields are just a short notation for q -mode and $-q$ -mode product.

Let us split radial and momentum dependence as follows:

$$V_\mu(q, r) = v_\mu(q) v(q, r), \quad A_\mu(q, r) = a_\mu(q) a(q, r). \quad (3.74)$$

(We can use residual gauge symmetry to gauge-fix $q^\mu V_\mu(q, \Lambda) = q^\mu A_\mu(q, \Lambda) = 0$.) Let us also split the action (3.73) to axial and vector parts:

$$S = S_V + S_A, \quad (3.75)$$

where

$$\begin{aligned} S_V = & - \frac{1}{4} \int d^4 q dr \frac{r^3}{\sqrt{1+r^2 \dot{T}_0^2}} V(T_0) v_\mu(q) v_\nu(-q) \\ & \times \left(\dot{v}_q(r) \dot{v}_{-q}(r) \eta^{\mu\nu} + \frac{q^2(1+r^2 \dot{T}_0^2)}{r^4} \left(\eta^{\mu\nu} - \frac{q^\mu q^\nu}{q^2} \right) v_q(r) v_{-q}(r) \right), \end{aligned} \quad (3.76)$$

$$\begin{aligned} S_A = & - \frac{1}{4} \int d^4 q dr \frac{r^3}{\sqrt{1+r^2 \dot{T}_0^2}} V(T_0) a_\mu(q) a_\nu(-q) (\dot{a}_q(r) \dot{a}_{-q}(r) \eta^{\mu\nu} \\ & + \frac{q^2(1+r^2 \dot{T}_0^2)}{r^4} \left(\eta^{\mu\nu} \left(1 + \frac{4T_0^2 r^2}{q^2} \right) - \frac{q^\mu q^\nu}{q^2} \right) a_q(r) a_{-q}(r)). \end{aligned} \quad (3.77)$$

We are interested in transverse components of gauge fields:

$$v_\mu^T(q) = P_{\mu\lambda} \eta^{\lambda\nu} v_\nu(q), \quad a_\mu^T(q) = P_{\mu\lambda} \eta^{\lambda\nu} a_\nu(q), \quad P_{\mu\nu} = \eta_{\mu\nu} - \frac{q_\mu q_\nu}{q^2}, \quad (3.78)$$

which are described by

$$S_V^T = -\frac{1}{4} \int d^4q dr \frac{r^3}{\sqrt{1+r^2\dot{T}_0^2}} V(T_0) v_\mu^T(q) v_\nu^T(-q) \eta^{\mu\nu} \quad (3.79)$$

$$\times \left(\dot{v}_q(r) \dot{v}_{-q}(r) + \frac{q^2(1+r^2\dot{T}_0^2)}{r^4} v_q(r) v_{-q}(r) \right),$$

$$S_A^T = -\frac{1}{4} \int d^4q dr \frac{r^3}{\sqrt{1+r^2\dot{T}_0^2}} V(T_0) a_\mu^T(q) a_\nu^T(-q) \eta^{\mu\nu} \quad (3.80)$$

$$\times \left(\dot{a}_q(r) \dot{a}_{-q}(r) + \frac{q^2(1+r^2\dot{T}_0^2)}{r^4} \left(1 + \frac{4T_0^2 r^2}{q^2} \right) a_q(r) a_{-q}(r) \right),$$

Corresponding equations of motion are

$$\ddot{v}_q(r) + \frac{\sqrt{1+r^2\dot{T}_0^2}}{r^3 V(T_0)} \frac{d}{dr} \left(\frac{r^3 V(T_0)}{\sqrt{1+r^2\dot{T}_0^2}} \right) \dot{v}_q(r)$$

$$- \frac{q^2(1+r^2\dot{T}_0^2)}{r^4} v_q(r) = 0, \quad (3.81)$$

$$\ddot{a}_q(r) + \frac{\sqrt{1+r^2\dot{T}_0^2}}{r^3 V(T_0)} \frac{d}{dr} \left(\frac{r^3 V(T_0)}{\sqrt{1+r^2\dot{T}_0^2}} \right) \dot{a}_q(r)$$

$$- \frac{q^2(1+r^2\dot{T}_0^2)}{r^4} \left(1 + \frac{4T_0^2 r^2}{q^2} \right) a_q(r) = 0. \quad (3.82)$$

We see that if there is no tachyon background, then equations of motion for vector and axial vector fields become the same.

We must ensure that near-horizon behavior of vector and axial vector fields is regular. The precise boundary conditions in the bulk depend strongly on the tachyon background. Below we consider concrete tachyon potentials and determine the corresponding boundary conditions. We also require

$$v(q, r = \infty) = 1, \quad a(q, r = \infty) = 1. \quad (3.83)$$

We solve equations of motion for $v(q, r)$ and $a(q, r)$ with these boundary conditions and plug the solutions into (3.79) and (3.80). As a result we

obtain (recall that at the boundary tachyon field vanishes)

$$S_V^{on-shell} = -\frac{1}{4} \int d^4q \Lambda^3 \eta^{\mu\nu} v_\mu^T(q) v_\nu^T(-q) \dot{v}(q, \Lambda), \quad (3.84)$$

$$S_A^{on-shell} = -\frac{1}{4} \int d^4q \Lambda^3 \eta^{\mu\nu} a_\mu^T(q) a_\nu^T(-q) \dot{a}(q, \Lambda). \quad (3.85)$$

Due to AdS/CFT correspondence

$$i \int d^4x e^{iqx} \langle j_V^\mu(x) j_V^\nu(0) \rangle = \frac{\delta^2 S_V^{on-shell}}{\delta v_\mu^T(q) \delta v_\nu^T(-q)} \Big|_{v=0}, \quad (3.86)$$

and similarly for the axial current. Consequently using (3.32) we get

$$\Pi_{\mu\nu}^V = P_{\mu\nu} \Pi_V(q^2) = \frac{\delta^2 S_V^{on-shell}}{\delta v_\mu^T(q) \delta v_\nu^T(-q)}. \quad (3.87)$$

Therefore correlation functions for vector and axial currents are given by

$$\Pi_V(q^2) = -\frac{1}{2} \Lambda^3 \dot{v}(q, \Lambda), \quad (3.88)$$

$$\Pi_A(q^2) = -\frac{1}{2} \Lambda^3 \dot{a}(q, \Lambda). \quad (3.89)$$

Propagators for vector and axial-vector currents in the field theory become the same if tachyon background vanishes. Non-vanishing tachyon background breaks chiral symmetry, and therefore generally speaking we have non-vanishing S parameter, defined as

$$S = -4\pi \frac{d}{dq^2} \left[\Pi_V(q^2) - \Pi_A(q^2) \right]_{q^2=0}. \quad (3.90)$$

With the help of holographic expressions (3.88) and (3.89) we obtain

$$S = 2\pi \Lambda^3 \frac{d}{dq^2} (\dot{v}(q^2, \Lambda) - \dot{a}(q^2, \Lambda)). \quad (3.91)$$

The infrared behavior is specific for each particular tachyon potential and we discuss it bellow. Now let us consider near-boundary region. In the near-boundary region $r \gg 1$ we can totally neglect tachyon field, which makes equations of motion for vector and axial vector fields the same:

$$\ddot{v} + \frac{3}{r} \dot{v} - \frac{q^2}{r^4} v = 0, \quad (3.92)$$

$$\ddot{a} + \frac{3}{r}\dot{a} - \frac{q^2}{r^4}a = 0. \quad (3.93)$$

In practical computations one has to make sure that the last term in (3.82) is small, $T_0^2 r^2 / q^2 \sim (q^2 r^2)^{-1} \ll 1$ in near-boundary region. This is important, because momentum q competes in smallness with $1/r$ when one is computing S parameter. Cutoff is supposed to be sent to infinity first, for each value of momentum q . The solutions to these equations, normalized by near-boundary condition (3.83), are

$$v = 1 - \frac{q^2}{2r^2} \log r + C_v \frac{1}{r^2}, \quad (3.94)$$

$$a = 1 - \frac{q^2}{2r^2} \log r + C_a \frac{1}{r^2}, \quad (3.95)$$

where $C_v(q^2)$ and $C_a(q^2)$ define asymptotic near-boundary behavior of the vector fields, have dimension two and go to finite constants when $q^2 = 0$. Therefore substituting (3.94) and (3.95) into (3.91) we find

$$S = 4\pi \frac{d}{dq^2} (C_a - C_v)|_{q^2=0}. \quad (3.96)$$

Notice that the S parameter is expressed only via the coefficients $C_{v,a}$, describing near-boundary behavior of vector and axial-vector gauge fields, and does not depend on the cutoff Λ .

Tachyon field describes chiral symmetry breaking at energy scale given holographically by $r \ll \mu$. In that region we have essentially different dynamics of axial vector and vector gauge fields. In what follows we measure all dimensionfull quantities in units of dynamically generated scale μ .

3.3.3 Soft Wall

Consider tachyon potential

$$V(T) = (1 + (A - 2)T^2)e^{-AT^2}, \quad (3.97)$$

with $A > 2$. Near the horizon in this potential tachyon field behaves as $T_0(r) = 1/r^{A/2}$. Correspondingly Lagrangian for vector field fluctuation is

$$L_v = r^{3-\frac{A}{2}} e^{-\frac{A}{rA}} \left(\dot{v}^2 + \frac{q^2 A^2}{4} r^{-A-4} v^2 \right). \quad (3.98)$$

It is useful to redefine

$$v = r^{\frac{A+2}{2}} e^{\frac{A}{2r^A}} \psi_v \quad (3.99)$$

and consider Lagrangian for ψ_v

$$L_v = r^{\frac{10+A}{2}} \dot{\psi}_v^2 + \frac{A^4}{4} r^{\frac{3(2-A)}{2}} \psi_v^2. \quad (3.100)$$

Solution of the corresponding equation of motion is a linear combination of Bessel functions $I_{\pm\alpha} \left(\frac{A}{2r^A} \right)$ times a power of r , of which the regular combination behaves as

$$\psi_v = r^{\frac{A}{4}-2} e^{-\frac{A}{2r^A}}. \quad (3.101)$$

Correspondingly

$$v = r^{\frac{3A}{4}-1}. \quad (3.102)$$

Near horizon Lagrangian for axial field is

$$L_a = r^{3-\frac{A}{2}} e^{-\frac{A}{r^A}} \left(\dot{a}^2 + \frac{A^2}{r^{2(A+1)}} a^2 \right). \quad (3.103)$$

It is convenient to make a redefinition

$$a = r^{\frac{A+2}{2}} e^{\frac{A}{2r^A}} \psi_a. \quad (3.104)$$

The near-horizon Lagrangian for axial field is now

$$L_a = r^{\frac{10+A}{2}} \dot{\psi}_a^2 + \frac{A^2(A^2+4)}{4} r^{\frac{3(2-A)}{2}} \psi_a^2. \quad (3.105)$$

Similarly to the case with vector field we choose the regular solution, which is

$$\psi_a = r^{\frac{A}{4}-2} \exp \left(-\frac{\sqrt{A^2+4}}{2r^A} \right). \quad (3.106)$$

Correspondingly near-horizon behavior of axial field is given by

$$a = r^{\frac{3A}{4}-1} \exp \left(-\frac{\sqrt{A^2+4}-A}{2r^A} \right). \quad (3.107)$$

To summarize: we have the following near-horizon boundary conditions:

$$T_0(r) = \frac{1}{r^{A/2}}, \quad v(r) = r^{\frac{3A}{4}-1}, \quad a(r) = r^{\frac{3A}{4}-1} \exp \left(-\frac{\sqrt{A^2+4}-A}{2r^A} \right). \quad (3.108)$$

We present results of numeric evaluations of the S parameter for different values of A in figure 3.

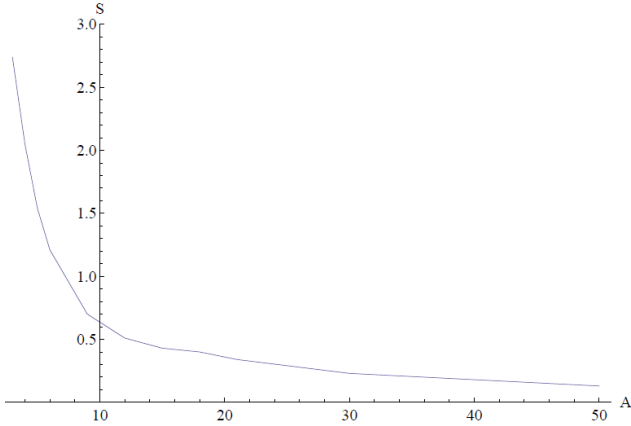


Figure 3.3. S parameter in the soft wall potential depending on the value of the parameter A .

3.3.4 Hard wall

Consider hard wall tachyon potential

$$V(T) = (\cos T)^4. \quad (3.109)$$

The IR regime of the field theory corresponds to the near hard wall region of AdS space, $r \simeq \mu$, where μ is the dynamically generated scale. Let us measure all dimensional quantities in units of μ . Then the hard wall is located at $r = 1$. When $r \simeq 1$, the tachyon field behaves as

$$T(r) \simeq \frac{\pi}{2} - c\sqrt{r-1}, \quad c = \sqrt{\frac{5}{2}}. \quad (3.110)$$

Plugging (3.110) into equations of motion for vector and axial-vector gauge fields, (3.81) and (3.82), and considering the region near $r = 1$, we obtain

$$\ddot{v} + \frac{5}{2(r-1)}\dot{v} - \frac{5q^2}{8(r-1)}v = 0 \quad (3.111)$$

$$\ddot{a} + \frac{5}{2(r-1)}\dot{a} - \frac{5(q^2 + \pi^2)}{8(r-1)}a = 0. \quad (3.112)$$

The solutions are given by

$$\begin{aligned} v &= \frac{c_1^v}{(r-1)^{1/2}} \left(1 + \frac{d_1}{r-1} \right) + c_2^v + \mathcal{O}(\sqrt{r-1}), \\ a &= \frac{c_1^a}{(r-1)^{1/2}} \left(1 + \frac{d_2}{r-1} \right) + c_2^a + \mathcal{O}(\sqrt{r-1}), \end{aligned} \quad (3.113)$$

where d_1 and d_2 stand for known functions of q^2 . We require momentum density T^{0r} to vanish at $r = 1$. The momentum density is given by (to compute it perturb the background metric by small g_{0r} and keep only terms of the action which are linear in g_{0r})

$$\begin{aligned} T^{0r} &\simeq \frac{1}{\sqrt{|g|}} \frac{\delta S}{\delta g_{0r}} \simeq \frac{V(T)}{\sqrt{1+r^2\dot{T}^2}} \eta^{ij} \left[\dot{V}_i F_{0j}^{(V)} + \dot{A}_i F_{0j}^{(A)} \right] \\ &\simeq (r-1)^{5/2} (v\dot{v} + a\dot{a}). \end{aligned} \quad (3.114)$$

We therefore choose the boundary conditions near the wall

$$v = 1, \quad a = 1. \quad (3.115)$$

Similarly as we have done in the soft wall case, we can now compute the S parameter. Numerics give $S \simeq 2.6$.

3.4 Lightest mesons

In this Section we compute the sigma-mesons spectrum in soft wall potential. Consider fluctuation of the tachyon field $\tau(r, t)$ around the vacuum configuration $T_0(r)$. Expanding the TDBI action

$$S = - \int d^4x dr V(T) r^3 \left(1 + r^2 (\dot{T}_0 + \dot{\tau})^2 - \frac{1}{r^2} (\partial_t \tau)^2 \right)^{1/2}. \quad (3.116)$$

we arrive at the action for fluctuation field

$$S = - \int d^3x d\omega dr \left(G(r) \dot{\tau}^2 + U(\tau) \tau^2 \right). \quad (3.117)$$

Perform a Fourier transform

$$\tau(r, t) = \int \frac{d\omega}{2\pi} \tau_\omega(r) e^{i\omega\tau}, \quad (3.118)$$

where $\omega^2 = m^2$ is the squared mass of the tachyon excitation mode. For the soft wall potential (we consider $A > 2$ to get a discrete spectrum of sigma-mesons, see [3] for details)

$$V(T) = (1 + (A - 2)T^2)e^{-AT^2} \quad (3.119)$$

we obtain

$$G(r) = \frac{e^{-AT_0^2} r^5 (1 + (A - 2)T_0^2)}{2(1 + r^2 \dot{T}_0^2)^{3/2}} \quad (3.120)$$

$$U(r) = \frac{\partial}{\partial r} \left(\frac{e^{-AT_0^2} r^5 T_0 \dot{T}_0 (2 + A(A - 2)T_0^2)}{\sqrt{1 + r^2 \dot{T}_0^2}} \right) \\ + e^{-AT_0^2} r^3 (-2 + AT_0^2 (10 - 3A + 2(A - 2)AT_0^2)) \sqrt{1 + r^2 \dot{T}_0^2} \quad (3.121) \\ - m^2 \frac{e^{-AT_0^2} r (1 + (A - 2)T_0^2)}{2\sqrt{1 + r^2 \dot{T}_0^2}}$$

Near the horizon $r = 0$ the background tachyon field behaves as $T_0 = \frac{1}{r^{A/2}}$. Therefore the Lagrangian for fluctuating field is

$$L = \frac{4}{A^2} r^{\frac{10+A}{2}} e^{-A/r^A} \dot{\tau}^2 - m^2 r^{\frac{2-A}{2}} e^{-A/r^A} \tau^2. \quad (3.122)$$

It is convenient to make a redefinition $\tau = e^{A/(2r^A)} \psi$ and consider the field ψ with the Lagrangian

$$L_\psi = r^{\frac{10+A}{2}} \dot{\psi}^2 + \frac{A^4}{4} r^{\frac{3(2-A)}{2}} \psi^2 \quad (3.123)$$

The solution of equation of motion for the field ψ is a linear combination of Bessel functions $I_{\pm\alpha}(A/(2r^A))$, times a power of r . We choose the regular combination of Bessel functions, which is

$$I_\alpha(A/(2r^A)) - I_{-\alpha}(A/(2r^A)) \simeq r^{A/2} e^{-A/(2r^A)}. \quad (3.124)$$

Corresponding near-horizon behavior of fluctuation tachyon field is

$$\tau(r) = r^{\frac{A}{4}-2}. \quad (3.125)$$

We therefore impose the near-horizon conditions

$$\tau(\epsilon) = 1, \quad \tau'(\epsilon) = \left(\frac{A}{4} - 2 \right) \frac{1}{\epsilon}. \quad (3.126)$$

We then integrate equation of motion for τ with these boundary conditions up to the near-boundary region. We fit the result with the expression

$$\tau(r) = \frac{1}{r^2}(c_1 \log r + c_2). \quad (3.127)$$

The ratio c_1/c_2 must be equal to this ratio for the background field T_0 . This determines the discrete mass spectrum of tachyon excitations.

We compute numerically the values m_1^2 and m_2^2 of the masses of the first two excitations as a function of the parameter A of the tachyon potential (3.119). We plot the result of numerics in figure 4.

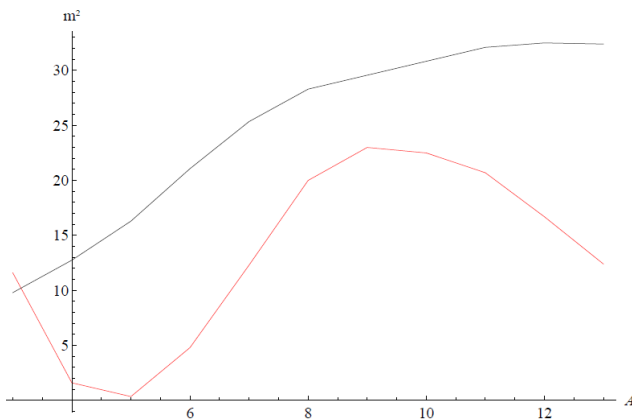


Figure 3.4. The values of of the masses of the first two excitations of the tachyon as a function of the parameter A of the tachyon potential (3.119). The m_1^2 (rescaled by a factor of ten) is plotted in red and the m_2^2 is plotted in black.

3.5 Conclusions

In this chapter we have considered strongly coupled systems which are described holographically by the tachyon DBI action in the AdS space-time. These models are renormalizable: the UV cutoff can be taken to infinity while the dynamically generated mass scale stays fixed. We investigated the phase diagram of these models at finite temperature and charge density. For smaller values of temperature and chemical potential the system resides in the phase with broken conformal symmetry. This phase is separated by a phase transition line from the phase with restored symmetry.

We observe that depending on the form of the tachyon potential, the order of the phase transition may change, and hence one or more critical point appears in the diagram. We have also used the TDBI action to describe holographically dynamical electroweak symmetry breaking. We have computed the S parameter using our holographic TDBI model for generic soft-wall tachyon potential, and for hard wall tachyon potential. The S-parameter takes generic positive values and does not appear to vanish in the parameter space that we investigated. We have also computed the masses of the lowest lying scalar mesons and observed that even though there is no parametrically light scalar, the lightest meson can be made at least an order of magnitude lighter than the next one.

3.6 Appendix: Conformal phase transition and double-trace coupling running

Consider a gauge field theory, coupled to matter fields with a single-trace UV Lagrangian. When we go to lower energies, integrating out higher momentum modes, we generally notice [55–57] that effective Wilsonian Lagrangian contains double-trace operators. We have to study the RG running of coupling constants for double-trace operators if we want to study the fate of the theory at low energies. Depending on the parameters defining the theory the beta-functions for double-trace operators can exhibit essentially different behavior; varying these parameters can lead to phase transitions between different IR phases of the theory. Here our focus will be on the particular type of these phase transitions, called conformal phase transitions in [58]. In this Section we review the field theory expectations for the physics associated with conformal phase transitions (CPT). We then use the technology of holographic Wilsonian RG to see how these expectations are reproduced in a particular holographic model based on the Tachyon DBI action in AdS space.

3.6.1 Conformal phase transitions and Wilsonian RG

Consider a gauge theory with $SU(N_c)$ gauge group, coupled to N_f massless Dirac fermions in the Veneziano limit, where both N_c and N_f are taken to infinity, with the ratio $x = N_f/N_c$ held fixed. It has a qualitatively different RG behavior depending on the value of x . Let us look at the IR effective field theory; three possible regimes can be identified.

When $x > 11/2$ the theory loses asymptotic freedom and is free in the IR; when $x_c < x < 11/2$, where $x_c \simeq 4$ (see e.g. [47]) is not known precisely, the IR theory is in the interacting Coulomb phase. This interval in x , where the theory flows to a conformal fixed point in the IR, is called “conformal window”. However for x smaller than x_c the IR theory acquires a mass gap and chiral symmetry is broken, due to the presence of chiral condensate.

The model studied in [57] is slightly different from the example above, but exhibits similar behavior. The advantage is that the beta function for the double-trace operator can be computed exactly [57]. Suppose that we have some strongly interacting theory, for which all single-trace operators have vanishing beta-functions, e.g., orbifold theories [59, 60] or non-supersymmetric deformations of $\mathcal{N} = 4$ super Yang-Mills theory [61]. To see whether the theory has conformal fixed points we therefore have to study double-trace couplings [55–57]. Denote by \mathcal{O} a single-trace operator, and consider a double trace term in the Lagrangian, $L_{dt} = f\mathcal{O}^2$, where f is a double-trace coupling constant. In [57] (and, earlier, to the one-loop level in [55, 56]) it has been shown that depending on the parameters of the theory the beta function for f either has a real zero (and then the theory flows to a conformal fixed point) or it does not (and then the theory generates a mass gap).

We will observe a similar behavior in the holographic model based on the tachyon DBI action in AdS space-time. First we introduce a bulk scalar field, dual to the field theory operator \mathcal{O} . We choose it to be the tachyon field T , described by the tachyon DBI action. Now, we want to study renormalization of the corresponding double-trace coupling f . We will use the holographic Wilsonian renormalization as described in [62].⁵ The full AdS action is written as a sum of the bulk action (in our case it is the tachyon DBI action), defined up to the cutoff Λ , and the boundary action at $r = \Lambda$,

$$S[T] = \int_0^\Lambda dr d^d x L_0[T] + \int d^d x L_B[T]_{r=\Lambda}. \quad (3.128)$$

To obtain holographically correlation functions that are invariant under the RG flow, one has to require invariance of the action S under the change of Λ : this is a holographic implementation of the Callan-Symanzik equation. The boundary term S_B encodes all degrees of freedom from

⁵See also [63].

the integrated out region $r > \Lambda$ of the AdS space, and is written down as a sum of multi-trace operators with corresponding coupling constants multiplying these operators. Solving for S_B the holographic RG (HRG) equation we determine running of the dual field theory coupling constants.

Below we apply this method to the tachyon-DBI action in the AdS space and find the RG behavior of the double-trace coupling f , depending on the mass m of the tachyon field. The non-vanishing tachyon field in the bulk is a preferred state when $m^2 < m_{BF}^2 = -\frac{d^2}{4}$ [3]. We conclude that f exhibits a walking behavior between the IR scale Λ_{IR} and the UV cutoff scale Λ_{UV} which are related as $\Lambda_{IR} = \Lambda_{UV} \exp\left(-\frac{\pi}{\sqrt{m_{BF}^2 - m^2}}\right)$. Such a relation confirms that our holographic model exhibits a conformal phase transition. This was also observed in [3], where a similar relation between the UV cutoff and the physical observables of the theory, such as e.g. meson masses, was established.

Finally we remind the reader what happens as the tachyon mass squared is lowered below the BF bound. According to the AdS/CFT dictionary, the dimension of the operator \mathcal{O} , dual to the tachyon field T , is given by

$$\Delta_{\pm} = \frac{d}{2} \pm \sqrt{\frac{d^2}{4} + m^2}. \quad (3.129)$$

The two possible scaling dimensions in (3.129), Δ_- and Δ_+ of the operator \mathcal{O} are realized in the two conformal fixed points: the UV and IR respectively. When we turn on a double-trace deformation $f\mathcal{O}^2$ in the UV theory, the theory flows to the IR conformal fixed point, where dimension of \mathcal{O} becomes equal to Δ_+ [64]. When the value of m^2 is lowered below $-d^2/4$, the two fixed points merge and then disappear, and the Miranski scaling emerges [2].

3.6.2 Double trace running from tachyon DBI

Consider the tachyon-DBI bulk action for the tachyon field $T(r)$ of the mass m , defined up to UV cutoff scale $r = \Lambda$ in AdS_{d+1} :

$$S_0 = - \int_0^{\Lambda} dr \int d^d x r^{d-1} V \sqrt{1 + r^2 \dot{T}^2}, \quad (3.130)$$

where tachyon potential is expanded around $T = 0$ as

$$V(T) = 1 + \frac{m^2 T^2}{2} + \dots, \quad (3.131)$$

and we denote differentiation w.r.t. r by dot. Suppose we integrate out all degrees of freedom in the bulk which correspond to $r > \Lambda$. Then we generate holographic Wilsonian effective action

$$S = S_0 + S_B[T, \Lambda], \quad (3.132)$$

where S_B is boundary term, which encodes integrated out degrees of freedom.

Boundary condition at $r = \Lambda$ is given by

$$\Pi = \frac{\partial S_B}{\partial T}, \quad (3.133)$$

where we have introduced momentum Π , canonically conjugate to the tachyon field T :

$$\Pi = -\frac{\delta S_0}{\delta T(r = \Lambda)} = \frac{\Lambda^{d+1} V \dot{T}}{\sqrt{1 + \Lambda^2 \dot{T}^2}}. \quad (3.134)$$

Using boundary condition (3.133) one may then express

$$\dot{T} = \frac{\partial S_B / \partial T}{\Lambda \sqrt{\Lambda^{2d} V^2 - (\partial S_B / \partial T)^2}}. \quad (3.135)$$

If we denote $S_0 = \int_{r_h}^{\Lambda} dr \int d^d x L_0$, then holographic RG equation is

$$\frac{\partial S_B}{\partial \Lambda} + L_0(r = \Lambda) + \frac{\partial S_B}{\partial T} \dot{T}(\Lambda) = 0. \quad (3.136)$$

With the help of (3.130) and (3.135) this eventually acquires the form

$$\frac{\partial S_B}{\partial \Lambda} = \Lambda^{d-1} V \sqrt{1 - \frac{1}{\Lambda^{2d} V^2} \left(\frac{\partial S_B}{\partial T} \right)^2}. \quad (3.137)$$

Action S_B implicitly contains boundary metric factor $\sqrt{-\det g_b} = \Lambda^d$. Let us make this factor explicit, defining dimensionless boundary action \mathcal{S} as

$$S_B = \Lambda^d \mathcal{S}. \quad (3.138)$$

Let us also define new cutoff coordinate,

$$\epsilon = \log \frac{\Lambda}{\mu}, \quad (3.139)$$

where μ is some constant, introduced for dimensional reasons. HRG equation (3.137) therefore gets rewritten as

$$\partial_\epsilon \mathcal{S} + d\mathcal{S} = V \sqrt{1 - \left(\frac{\partial_T \mathcal{S}}{V}\right)^2}. \quad (3.140)$$

Let us expand the boundary action as

$$\mathcal{S} = C(\epsilon) + J(\epsilon)T + \frac{1}{2}f(\epsilon)T^2. \quad (3.141)$$

Plugging it into (3.140) and matching terms of the same order in T , we obtain

$$\partial_\epsilon C = \sqrt{1 - J^2} - dC, \quad (3.142)$$

$$\partial_\epsilon J = -\frac{fJ}{\sqrt{1 - J^2}} - dJ, \quad (3.143)$$

$$\partial_\epsilon f = \frac{m^2}{\sqrt{1 - J^2}} - \frac{f^2}{(1 - J^2)^{3/2}} - df. \quad (3.144)$$

We can solve these equations by putting $J \equiv 0$ and making $\bar{f} = -(f + d/2)$ satisfy equation

$$\partial_\epsilon \bar{f} = \bar{f}^2 - \frac{d^2}{4} - m^2. \quad (3.145)$$

Let us denote $\kappa^2 = -\frac{d^2}{4} - m^2 \equiv m_{BF}^2 - m^2$, then solution to (3.145) may be written as

$$\bar{f} = \kappa \tan(\kappa \epsilon). \quad (3.146)$$

We conclude that double-trace coupling \bar{f} exhibits a walking behavior between UV scale

$$\Lambda_{UV} = \mu \exp\left(\frac{\pi}{2\kappa}\right) \quad (3.147)$$

and IR scale

$$\Lambda_{IR} = \mu \exp\left(-\frac{\pi}{2\kappa}\right). \quad (3.148)$$

Bibliography

- [1] B. Rosenstein, B. Warr and S. H. Park, “Dynamical symmetry breaking in four Fermi interaction models,” *Phys. Rept.* **205** (1991) 59.
- [2] D. B. Kaplan, J. -W. Lee, D. T. Son and M. A. Stephanov, “Conformality Lost,” *Phys. Rev. D* **80** (2009) 125005 [arXiv:0905.4752 [hep-th]].
- [3] D. Kutasov, J. Lin and A. Parnachev, “Holographic Walking from Tachyon DBI,” *Nucl. Phys. B* **863** (2012) 361 [arXiv:1201.4123 [hep-th]].
- [4] D. Kutasov, J. Lin and A. Parnachev, “Conformal Phase Transitions at Weak and Strong Coupling,” *Nucl. Phys. B* **858** (2012) 155 [arXiv:1107.2324 [hep-th]].
- [5] M. A. Stephanov, “QCD phase diagram and the critical point,” *Prog. Theor. Phys. Suppl.* **153** (2004) 139 [*Int. J. Mod. Phys. A* **20** (2005) 4387] [hep-ph/0402115].
- [6] R. Casalbuoni, “QCD critical point: A Historical perspective,” *PoS CPOD* **2006** (2006) 001 [hep-ph/0610179].
- [7] T. Alho, M. Järvinen, K. Kajantie, E. Kiritsis and K. Tuominen, “On finite-temperature holographic QCD in the Veneziano limit,” *JHEP* **1301** (2013) 093 [arXiv:1210.4516 [hep-ph]].
- [8] N. Evans, “Holographic Description of the QCD Phase Diagram and Out of Equilibrium Dynamics,” arXiv:1209.0626 [hep-ph].
- [9] S. R. Coleman and E. Witten, “Chiral Symmetry Breakdown in Large N Chromodynamics,” *Phys. Rev. Lett.* **45** (1980) 100.

- [10] M. Piai, “Lectures on walking technicolor, holography and gauge/gravity dualities,” *Adv. High Energy Phys.* **2010** (2010) 464302 [arXiv:1004.0176 [hep-ph]].
- [11] M. E. Peskin and T. Takeuchi, “A New constraint on a strongly interacting Higgs sector,” *Phys. Rev. Lett.* **65** (1990) 964.
- [12] M. E. Peskin and T. Takeuchi, “Estimation of oblique electroweak corrections,” *Phys. Rev. D* **46** (1992) 381.
- [13] D. C. Kennedy and B. W. Lynn, “Electroweak Radiative Corrections with an Effective Lagrangian: Four Fermion Processes,” *Nucl. Phys. B* **322** (1989) 1.
- [14] M. E. Peskin and D. V. Schroeder, “An Introduction to quantum field theory,” Reading, USA: Addison-Wesley (1995) 842 p
- [15] D. K. Hong and H. -U. Yee, “Holographic estimate of oblique corrections for technicolor,” *Phys. Rev. D* **74** (2006) 015011 [hep-ph/0602177].
- [16] J. Hirn and V. Sanz, “A Negative S parameter from holographic technicolor,” *Phys. Rev. Lett.* **97** (2006) 121803 [hep-ph/0606086].
- [17] M. Piai, “Precision electro-weak parameters from AdS(5), localized kinetic terms and anomalous dimensions,” hep-ph/0608241.
- [18] C. D. Carone, J. Erlich and J. A. Tan, “Holographic Bosonic Technicolor,” *Phys. Rev. D* **75** (2007) 075005 [hep-ph/0612242].
- [19] K. Agashe, C. Csaki, C. Grojean and M. Reece, “The S-parameter in holographic technicolor models,” *JHEP* **0712** (2007) 003 [arXiv:0704.1821 [hep-ph]].
- [20] C. D. Carone, J. Erlich and M. Sher, “Holographic Electroweak Symmetry Breaking from D-branes,” *Phys. Rev. D* **76** (2007) 015015 [arXiv:0704.3084 [hep-th]].
- [21] R. Casalbuoni, S. De Curtis, D. Dominici and D. Dolce, “Holographic approach to a minimal Higgsless model,” *JHEP* **0708** (2007) 053 [arXiv:0705.2510 [hep-ph]].

- [22] T. Hirayama and K. Yoshioka, “Holographic Construction of Technicolor Theory,” JHEP **0710** (2007) 002 [arXiv:0705.3533 [hep-ph]].
- [23] C. D. Carone, J. Erlich and M. Sher, “Extra Gauge Invariance from an Extra Dimension,” Phys. Rev. D **78** (2008) 015001 [arXiv:0802.3702 [hep-ph]].
- [24] M. Fabbrichesi, M. Piai and L. Vecchi, “Dynamical electro-weak symmetry breaking from deformed AdS: Vector mesons and effective couplings,” Phys. Rev. D **78** (2008) 045009 [arXiv:0804.0124 [hep-ph]].
- [25] F. Sannino, “Dynamical Stabilization of the Fermi Scale: Phase Diagram of Strongly Coupled Theories for (Minimal) Walking Technicolor and Unparticles,” arXiv:0804.0182 [hep-ph].
- [26] K. Haba, S. Matsuzaki and K. Yamawaki, “S Parameter in the Holographic Walking/Conformal Technicolor,” Prog. Theor. Phys. **120** (2008) 691 [arXiv:0804.3668 [hep-ph]].
- [27] D. D. Dietrich and C. Kouvaris, “Constraining vectors and axial-vectors in walking technicolour by a holographic principle,” Phys. Rev. D **78** (2008) 055005 [arXiv:0805.1503 [hep-ph]].
- [28] D. D. Dietrich and C. Kouvaris, “Generalised bottom-up holography and walking technicolour,” Phys. Rev. D **79** (2009) 075004 [arXiv:0809.1324 [hep-ph]].
- [29] C. Nunez, I. Papadimitriou and M. Piai, “Walking Dynamics from String Duals,” Int. J. Mod. Phys. A **25** (2010) 2837 [arXiv:0812.3655 [hep-th]].
- [30] O. Mintakevich and J. Sonnenschein, “Holographic technicolor models and their S-parameter,” JHEP **0907** (2009) 032 [arXiv:0905.3284 [hep-th]].
- [31] H. S. Fukano and F. Sannino, “Minimal flavor constraints for technicolor,” Nucl. Phys. Proc. Suppl. **209** (2010) 176.
- [32] N. Kitazawa, “Dynamical Electroweak Symmetry Breaking in String Models with D-branes,” Int. J. Mod. Phys. A **25** (2010) 2679 [arXiv:0908.2663 [hep-th]].

- [33] D. D. Dietrich, M. Jarvinen and C. Kouvaris, “Mixing in the axial sector in bottom-up holography for walking technicolor,” *JHEP* **1007** (2010) 023 [arXiv:0908.4357 [hep-ph]].
- [34] A. V. Belitsky, “Dual technicolor with hidden local symmetry,” *Phys. Rev. D* **82** (2010) 045006 [arXiv:1003.0062 [hep-ph]].
- [35] C. D. Carone and R. Primulando, “Combined Constraints on Holographic Bosonic Technicolor,” *Phys. Rev. D* **82** (2010) 015003 [arXiv:1003.4720 [hep-ph]].
- [36] M. Reece and L. -T. Wang, “Randall-Sundrum and Strings,” *JHEP* **1007** (2010) 040 [arXiv:1003.5669 [hep-ph]].
- [37] K. Haba, S. Matsuzaki and K. Yamawaki, “Holographic Technidilaton,” *Phys. Rev. D* **82** (2010) 055007 [arXiv:1006.2526 [hep-ph]].
- [38] L. Anguelova, “Electroweak Symmetry Breaking from Gauge/Gravity Duality,” *Nucl. Phys. B* **843** (2011) 429 [arXiv:1006.3570 [hep-th]].
- [39] M. Round, “Generalised Holographic Electroweak Symmetry Breaking Models and the Possibility of Negative S,” *Phys. Rev. D* **84** (2011) 013012 [arXiv:1104.4037 [hep-ph]].
- [40] L. Anguelova, P. Suranyi and L. C. R. Wijewardhana, “Holographic Walking Technicolor from D-branes,” *Nucl. Phys. B* **852** (2011) 39 [arXiv:1105.4185 [hep-th]].
- [41] U. I. Sondergaard, C. Pica and F. Sannino, “S-parameter at Non-Zero Temperature and Chemical Potential,” *Phys. Rev. D* **84** (2011) 075022 [arXiv:1107.1802 [hep-ph]].
- [42] D. G. Levkov, V. A. Rubakov, S. V. Troitsky and Y. A. Zenkevich, “Constraining Holographic Technicolor,” *Phys. Lett. B* **716** (2012) 350 [arXiv:1201.6368 [hep-ph]].
- [43] L. Anguelova, P. Suranyi and L. C. R. Wijewardhana, “Scalar Mesons in Holographic Walking Technicolor,” *Nucl. Phys. B* **862** (2012) 671 [arXiv:1203.1968 [hep-th]].
- [44] C. D. Carone, “Technicolor with a 125 GeV Higgs Boson,” *Phys. Rev. D* **86** (2012) 055011 [arXiv:1206.4324 [hep-ph]].

- [45] R. Lawrance and M. Piai, “Holographic Technidilaton and LHC searches,” *Int. J. Mod. Phys. A* **28** (2013) 1350081 [arXiv:1207.0427 [hep-ph]].
- [46] D. Elander and M. Piai, “The decay constant of the holographic techni-dilaton and the 125 GeV boson,” *Nucl. Phys. B* **867** (2013) 779 [arXiv:1208.0546 [hep-ph]].
- [47] M. Jarvinen and E. Kiritsis, “Holographic Models for QCD in the Veneziano Limit,” *JHEP* **1203** (2012) 002 [arXiv:1112.1261 [hep-ph]].
- [48] R. Alvares, N. Evans and K. -Y. Kim, “Holography of the Conformal Window,” *Phys. Rev. D* **86** (2012) 026008 [arXiv:1204.2474 [hep-ph]].
- [49] S. Matsuzaki and K. Yamawaki, “Is 125 GeV techni-dilaton found at LHC?,” *Phys. Lett. B* **719** (2013) 378 [arXiv:1207.5911 [hep-ph]].
- [50] N. Evans, J. French and K. -Y. Kim, “Inflation from Strongly Coupled Gauge Dynamics,” arXiv:1208.3060 [hep-th].
- [51] S. Matsuzaki and K. Yamawaki, “Holographic techni-dilaton at 125 GeV,” *Phys. Rev. D* **86** (2012) 115004 [arXiv:1209.2017 [hep-ph]].
- [52] Z. Chacko, R. Franceschini and R. K. Mishra, “Resonance at 125 GeV: Higgs or Dilaton/Radion?,” *JHEP* **1304** (2013) 015 [arXiv:1209.3259 [hep-ph]].
- [53] B. Bellazzini, C. Csaki, J. Hubisz, J. Serra and J. Terning, “A Higgslike Dilaton,” *Eur. Phys. J. C* **73** (2013) 2333 [arXiv:1209.3299 [hep-ph]].
- [54] R. Casero, E. Kiritsis and A. Paredes, “Chiral symmetry breaking as open string tachyon condensation,” *Nucl. Phys. B* **787** (2007) 98 [hep-th/0702155 [HEP-TH]].
- [55] A. Dymarsky, I. R. Klebanov and R. Roiban, “Perturbative search for fixed lines in large N gauge theories,” *JHEP* **0508** (2005) 011 [hep-th/0505099].

- [56] A. Dymarsky, I. R. Klebanov and R. Roiban, “Perturbative gauge theory and closed string tachyons,” *JHEP* **0511** (2005) 038 [hep-th/0509132].
- [57] E. Pomoni and L. Rastelli, “Large N Field Theory and AdS Tachyons,” *JHEP* **0904** (2009) 020 [arXiv:0805.2261 [hep-th]].
- [58] V. A. Miransky and K. Yamawaki, “Conformal phase transition in gauge theories,” *Phys. Rev. D* **55** (1997) 5051 [Erratum-ibid. *D* **56** (1997) 3768] [hep-th/9611142].
- [59] S. Kachru and E. Silverstein, “4-D conformal theories and strings on orbifolds,” *Phys. Rev. Lett.* **80** (1998) 4855 [hep-th/9802183].
- [60] A. E. Lawrence, N. Nekrasov and C. Vafa, “On conformal field theories in four-dimensions,” *Nucl. Phys. B* **533** (1998) 199 [hep-th/9803015].
- [61] O. Lunin and J. M. Maldacena, “Deforming field theories with $U(1) \times U(1)$ global symmetry and their gravity duals,” *JHEP* **0505** (2005) 033 [hep-th/0502086].
- [62] T. Faulkner, H. Liu and M. Rangamani, “Integrating out geometry: Holographic Wilsonian RG and the membrane paradigm,” *JHEP* **1108** (2011) 051 [arXiv:1010.4036 [hep-th]].
- [63] I. Heemskerck and J. Polchinski, “Holographic and Wilsonian Renormalization Groups,” *JHEP* **1106** (2011) 031 [arXiv:1010.1264 [hep-th]].
- [64] E. Witten, “Multitrace operators, boundary conditions, and AdS / CFT correspondence,” hep-th/0112258.